J. Math. Biol. (1999) 39: 533–561

Journal of Mathematical Biology

Transport effects on surface–volume biological reactions

David A. Edwards[1], **Byron Goldstein**[2], **Donald S. Cohen**[3,⋆]

[1] Department of Mathematical Sciences, 501 Ewing Hall, University of Delaware, Newark, DE 19716-2553, USA. e-mail: edwards@math.udel.edu
[2] Theoretical Biology and Biophysics Group, Los Alamos National Laboratory, Los Alamos, NM 87545, USA. e-mail: bxg@lanl.gov
[3] Applied Mathematics Option, California Institute of Technology, Pasadena, CA 91125, USA. e-mail: dscohen@cco.caltech.edu

Received 11 May 1998 / Revised version: 29 March 1999

Abstract. Many cellular reactions involve a reactant in solution binding to or dissociating from a reactant confined to a surface. This is true as well for a BIAcore™, an optical biosensor that is widely used to study the interaction of biomolecules. In the flow cell of this instrument, one of the reactants is immobilized on a flat sensor surface while the other reactant flows past the surface. Both diffusion and convection play important roles in bringing the reactants into contact. Usually BIAcore™ binding data are analyzed using well known expressions that are valid only in the reaction-limited case when the Damköhler number Da is small. Asymptotic and singular perturbation techniques are used to analyze dissociation of the bound state when Da is small and $O(1)$. Linear and nonlinear integral equations result from the analysis; explicit and asymptotic solutions are constructed for physically realizable cases. In addition, effective rate constants are derived that illustrate the effects of transport on the measured rate constants. All these expressions provide a direct way to estimate the rate constants from BIAcore™ binding data.

Correspondence to: David A. Edwards

⋆ Prof. Cohen was supported in part by the National Science Foundation Grant DMS-9501511, and the Department of Energy grant W-7405-ENG-36 at the Center for Nonlinear Studies and Advanced Computing Laboratories at Los Alamos. Byron Goldstein was supported in part through the Los Alamos National Laboratory LDRD program.

Key words: Biomolecular reactions – Rate constants – Singular perturbations – Asymptotics – Integral equations

1. Introduction

Many chemical reactions of interest in biological systems are two-component reactions involving a reactant confined to a surface and a reactant dispersed in a volume. For instance, the cytoplasmic tails of receptors embedded in the plasma membrane interact with signaling and adapter molecules in the cytoplasm [3]. Maternal immunoglobulins are transmitted via mother's milk to the circulation of a newborn through binding to receptors on intestinal epithelial cells [10]. Gene expression is significantly influenced by DNA-protein interactions in these geometries [11].

In order to understand such reactions better, accurate measurements of the rate constants that describe the reactions are required. For example, for a monovalent ligand interacting with a binding site on a receptor, one needs to determine the association rate constant $\tilde{k}_a$ and the dissociation rate constant $\tilde{k}_d$ for the reaction. The BIAcore™ is a popular device that uses the optical phenomenon of surface plasmon resonance (SPR) to provide real-time measurements of binding from which rate constants can be determined. The configuration of the BIAcore™ is described in great detail elsewhere [4, 11]. For our purposes, it is sufficient to know that the device consists of a rectangular channel through which one of the reactants (the analyte) flows. The other reactant, to which we refer as the receptor (also called the immobilized ligand), is coupled to the sensor surface on the ceiling of the channel, and real-time measurements of the mass change at the sensor surface are made as the reaction proceeds and bound-state complexes are formed and break up.

The rate constants may be calculated from the BIAcore™ data once an appropriate mathematical model has been formulated. Though the full mathematical model includes a convection-diffusion system coupled with the reaction at the surface, most authors decouple the reaction kinetics from the transport dynamics. When one does so, the standard chemical kinetic equations that describe a bimolecular interaction occuring in a well mixed system result, and they are easily solved in terms of exponentials [9]. Unfortunately, this decoupling is valid only when the parameter values are in certain ranges [4].

If the parameters do not fall in these ranges, transport effects must be included in the analysis. Rather than modeling the full

convection-diffusion system, some authors prefer to introduce a new "mass transfer coefficient" to account for diffusive effects [4, 7]. There have been some numerical simulations [2, 8] and modeling [5] of all the dynamics in similar systems, but few analytical studies have been undertaken.

Following the work in association kinetics in [1], we consider the full convection-diffusion system for dissociation kinetics. Using perturbation techniques, we reduce the full set of equations to an integrodifferential equation at the boundary. If the Damköhler number (Da) is small, the transport and kinetic effects decouple and the equations reduce to the well-known case. Using Da as a small parameter, we construct the first-order correction to the reaction-limited case caused by small transport effects. The form of the regular expansions suggests a multiple-scale expansion, which is also constructed.

However, due to the nature of the BIAcore™ device, it is often difficult to design an experiment where $\mathrm{Da} = o(1)$. Therefore, we also analyze the system when $\mathrm{Da} = O(1)$ and diffusion and reaction effects balance. A nonlinear integral equation results, but the rate constants can easily be estimated from a short-time solution for the bound-state concentration.

Due to the nature of the underlying operator, a series solution may be constructed for the bound concentration in all cases, though the convergence is faster when $\mathrm{Da} \ll 1$. The first several terms in this series are derived for both association and dissociation kinetics, and it is shown how this series can lead to a simple ordinary differential evolution equation. This equation is asymptotic to the true solution to leading two orders, and an excellent approximation to leading three orders. In addition, the ODE has coefficients that can easily be interpreted as effective rate constants, which show how transport effects perturb the interpretation of measured data.

2. Governing equations

Because the width of a BIAcore™ flow cell is ten times wider than its height, the BIAcore™ flow cell can be modeled as a two-dimensional channel, closed at top and bottom, with length L and height h. Analyte molecules are convected down the channel in a standard two-dimensional Poiseuille flow with maximal velocity $V/4$. Receptor molecules are embedded along the channel ceiling and real-time measurements of the progress of the reaction are taken via measurements of reflected light [11].

The proper dimensionless governing equations for the model have already been derived [1]. The analyte flow is governed by

$$\frac{\partial C}{\partial t_c} = \mathrm{Pe}^{-1}\left(\varepsilon^2 \frac{\partial^2 C}{\partial x^2} + \frac{\partial^2 C}{\partial y^2}\right) - y(1-y)\frac{\partial C}{\partial x}, \quad 0 \leqq x \leqq 1,\ 0 \leqq y \leqq 1, \quad (2.1)$$

where C is the dimensionless form of the analyte concentration normalized by C_T, the upstream concentration imposed during the association part of the experiment, t_c is the convective time scale (i.e., $t_c = V\tilde{t}/L$, where $\tilde{t}$ is the time since the start of the experiment), x is the normalized distance along the channel, y is the normalized distance below the reacting surface, and $\varepsilon = h/L$ is the aspect ratio of the channel, which will always be considered small. (For more detailed analysis of parameter sizes, see [1].) Pe is the Peclét number for the system, which will always be considered large:

$$\frac{\tilde{D}/h^2}{V/L} = \left(\frac{\text{convective rate of mass transfer}}{\text{diffusive rate of mass transfer}}\right)^{-1} \equiv \mathrm{Pe}^{-1}, \quad (2.2)$$

where $\tilde{D}$ is the molecular diffusion coefficient for the analyte.

The concentration of the analyte does not change as it exits the channel ($x = 1$), and there is no diffusive flux through the floor of the channel ($y = 1$):

$$\frac{\partial C}{\partial x}(1, y, t_c) = 0, \quad (2.3)$$

$$\frac{\partial C}{\partial y}(x, 1, t_c) = 0. \quad (2.4)$$

At the binding surface $y = 0$, the flux into the surface is equal to the rate of change of the bound receptor concentration:

$$\frac{\partial B}{\partial t_c} = D\frac{\partial C}{\partial y}(x, 0, t_c), \qquad D \equiv \frac{\tilde{D}C_T/R_T h}{V/L}, \quad (2.5)$$

where B is the bound receptor concentration normalized by R_T, the total number of receptor sites, and D (always considered to be small) is a normalized diffusion coefficient. The binding itself is governed by a Malthusian dissociation term and a bimolecular production term:

$$\frac{\partial B}{\partial t_c} = k_a[(1-B)C(x, 0, t_c) - KB], \qquad k_a = \frac{\tilde{k}_a C_T L}{V}, \qquad K = \frac{\tilde{k}_d}{\tilde{k}_a C_T}. \quad (2.6)$$

Here K is a dimensionless form of the equilibrium dissociation constant for the system, $\tilde{k}_a$ is the *association rate constant*, and $\tilde{k}_d$ is the

dissociation rate constant. Also of interest is the dimensional equilibrium dissociation constant for the system, which is given by

$$\tilde{K} = KC_{\mathrm{T}} = \frac{\tilde{k}_{\mathrm{d}}}{\tilde{k}_{\mathrm{a}}}. \tag{2.7}$$

3. Dissociation kinetics

In Sects. 4 and 5 of this paper, we present two new ways of analyzing this problem: namely, effective rate constants and series solutions. We wish to compare the results thus obtained in the case of dissociation kinetics with those derived with more standard techniques, which we present in this section.

Due to the underlying linear nature of the transport equation (2.1) for C, the analysis is quite analogous to that in [1], which treats the case of association kinetics only. Therefore, we summarize the analysis in [1] (to which the interested reader is directed for the details), pointing out those features that are different in the dissociation problem.

In the dissociation phase of the experiment, there is no analyte entering the channel:

$$C(0, y, t_{\mathrm{c}}) = 0. \tag{3.1}$$

We assume that binding is allowed to proceed long enough for a steady state to be established before dissociation is initiated. Thus, for initial conditions we use the steady-state solutions from the association phase [1]:

$$C(x, y, 0) = 1, \tag{3.2a}$$

$$B(x, 0) = \frac{1}{\alpha}, \qquad \alpha = K + 1. \tag{3.2b}$$

Since the Peclét number is large in these systems, on the convective time scale t_{c} the analyte concentration C quickly equilibrates to $C \equiv 0$ throughout most of the channel. This convective time scale is much faster than the reaction time scale, and thus B remains at its initial value on this time scale.

In the so-called "unstirred" boundary layer near the reacting surface, the effects of convection and diffusion balance. Therefore, C equilibrates on a slower diffusive time scale. The relevant scalings for time and space are given by

$$t_D = \mathrm{Pe}^{-1/3} t_{\mathrm{c}}, \qquad \eta = \mathrm{Pe}^{1/3} y, \tag{3.3a}$$

$$C(x, y, t_{\mathrm{c}}) = C_D(x, \eta, t_D), \qquad B(x, t_{\mathrm{c}}) = B_D(x, t_D), \tag{3.3b}$$

where the subscript D indicates that we are now using the diffusive time scale. (This agrees with the scaling in [5].)

Substituting Eqs. (3.3) into Eqs. (2.5) and (2.6), we obtain the following, to leading orders:

$$\frac{\partial B_D}{\partial t_D} = D_D \frac{\partial C_D}{\partial \eta}(x, 0, t_D), \quad D_D \equiv D\mathrm{Pe}^{2/3}, \tag{3.4a}$$

$$\frac{\partial B_D}{\partial t_D} = k_a \mathrm{Pe}^{1/3}\Big[(1 - B_D)C_D(x, 0, t_D) - KB_D\Big]. \tag{3.4b}$$

Combining Eqs. (3.4), we have

$$\frac{\partial C_D}{\partial \eta}(x, 0, t_D) = \mathrm{Da}[(1-B_D)C_D(x, 0, t_D) - KB_D], \quad \mathrm{Da} \equiv \frac{k_a \mathrm{Pe}^{1/3}}{D_D}. \tag{3.5}$$

Here Da is the Damköhler number for the system, which measures the ratio of the reaction rate to the diffusion rate.

In the physically realizable cases we wish to consider, either $\mathrm{Da} \ll 1$ or $D_D \ll 1$. Therefore, we see from either (3.4a) or (3.5) that the bound state does not involve on this time scale, either. Since the evolution of the bound state occurs on a slower time scale than t_D, we introduce the following new variables, including the reaction time scale t:

$$t = k_a \mathrm{Pe}^{1/3} t_D = \tilde{k}_a C_T \tilde{t}, \tag{3.6a}$$

$$C(x, y, t_c) = C_k(x, \eta, t) + o(1), \qquad B(x, t_c) = B_k(x, t) + o(1), \tag{3.6b}$$

where $k_a \mathrm{Pe}^{1/3} \ll 1$. In Eqs. (3.6) we have omitted a subscript on t for notational simplicity, since it is this time scale, on which the reaction occurs, that will be of the most interest.

Substituting Eqs. (3.6) into Eqs. (2.1), (3.1), (3.2b), (2.5), and (2.6), we obtain, to leading orders,

$$\eta \frac{\partial C_k}{\partial x} = \frac{\partial^2 C_k}{\partial \eta^2}, \tag{3.7}$$

$$C_k(0, \eta, t) = 0, \qquad C_k(x, \infty, t) = 0, \tag{3.8}$$

$$B_k(x, 0) = \frac{1}{\alpha}, \tag{3.9}$$

$$\frac{\partial C_k}{\partial \eta}(x, 0, t) = \mathrm{Da} \frac{\partial B_k}{\partial t}, \tag{3.10}$$

$$\frac{\partial B_k}{\partial t} = (1 - B_k)C_k(x, 0, t) - KB_k. \tag{3.11}$$

where the second equation in (3.8) arises from matching the analyte concentration in the unstirred layer to that in the channel.

The BIAcore™ device measures the quantity

$$\bar{B}_k(t) = \frac{1}{x_{max} - x_{min}} \int_{x_{min}}^{x_{max}} B_k(x, t)\, dx, \tag{3.12}$$

where x_{min} is a finite distance away from 0 and x_{max} is a finite distance away from 1. The nature of the operator in Eq. (3.7) indicates that a boundary layer would be necessary near $x = 1$ to smooth the transition between the solution to Eq. (3.7) and the boundary condition arising from Eq. (2.3). Since this boundary layer is outside the range of measurement for the BIAcore™, we did not substitute the new variables into Eq. (2.3), and we shall neglect consideration of it in all further analysis.

The solutions to our system will depend on the parameters K and t, which itself depends on k_a. Therefore, we see that by taking measurements of $\bar{B}$ and comparing the results with our solutions, we shall obtain estimates for K and k_a. Since C_T is known for each experiment, one can easily estimate $\tilde{k}_a$ and $\tilde{k}_d$, which is the end goal of this process.

In the following two sections we examine two cases of physical interest. The case names are those given in [1].

3.1. *Case 1 (*Da $\ll$ 1*)*

The leading-order behavior of the bound concentration is easy to deduce, as others have done [9]. Unfortunately, in order to get measurable readings from the BIAcore™, it is usually necessary to increase R_T. Since Da $\propto R_T$, the resulting increase in Da can reduce the effectiveness of the leading-order expansion at predicting rate constants. Therefore, we shall calculate the first *two* orders of the bound concentration in the limit of small Da. This added term in the expansion will allow us to increase the range of Da for which our expansion is valid.

We note from (3.10) that in the case of small Da, the reaction rate does not contribute an $O(1)$ flux of analyte, and thus to leading order C_k, which has equilibrated to zero on the diffusive time scale, is undisturbed. Therefore, we write our solutions in the following series:

$$\begin{aligned} C_k(x, \eta, t) &= \mathrm{Da} C_1(x, \eta, t) + o(\mathrm{Da}), \\ B_k(x, t) &= B_0(x, t) + \mathrm{Da} B_1(x, t) + o(\mathrm{Da}). \end{aligned} \tag{3.13}$$

Since to leading order there is no analyte to drive a forward reaction, the equation for B_0 contains only the dissociation term:

$$\frac{\partial B_0}{\partial t} = -KB_0, \tag{3.14a}$$

$$\frac{d\bar{B}_0}{d\tilde{t}} = -\tilde{k}_d \bar{B}_0, \tag{3.14b}$$

where the latter equation is in dimensional form and we have used Eq. (2.7). Note that a plot of $d\bar{B}_0/d\tilde{t}$ vs. $\bar{B}_0$ will yield a straight line with slope $\tilde{k}_d$, which is consistent with the dominance of dissociation. Solving Eq. (3.14a) subject to Eq. (3.9), we find that

$$B_0(x, t) = \frac{e^{-Kt}}{\alpha} = \bar{B}_0(t). \tag{3.15}$$

Of course, this is the standard type of exponential behavior one would expect from Eq. (3.14a).

Substituting Eqs. (3.13) into Eqs. (3.7)–(3.11), we obtain the following equations for B_1 and C_1:

$$\eta \frac{\partial C_1}{\partial x} = \frac{\partial^2 C_1}{\partial \eta^2}, \qquad C_1(0, \eta, t) = 0, \qquad C_1(x, \infty, t) = 0, \tag{3.16}$$

$$\frac{\partial C_1}{\partial \eta}(x, 0, t) = \frac{\partial B_0}{\partial t}, \tag{3.17}$$

$$C_1(x, 0, t) = \frac{1}{1 - B_0}\left(\frac{\partial B_1}{\partial t} + KB_1\right), \tag{3.18}$$

$$B_1(x, 0) = 0. \tag{3.19}$$

To derive a solution, we introduce a Laplace transform in x into Eqs. (3.16) and (3.18). The solution of the transformed equations is an Airy function whose derivative at $\eta = 0$ can be readily computed. We then substitute this result into the Laplace transform of Eq. (3.17). The resulting expression may be manipulated and inverted to yield

$$\frac{1}{1 - B_0}\left(\frac{\partial B_1}{\partial t} + KB_1\right) = \frac{K}{3^{1/3}\Gamma(2/3)} \int_0^x B_0(x - \xi, t) \frac{d\xi}{\xi^{2/3}}. \tag{3.20}$$

Since B_0 is independent of x, the equation immediately simplifies to

$$\frac{\partial B_1}{\partial t} + KB_1 = \frac{3^{2/3} K x^{1/3}}{\Gamma(2/3)} B_0(1 - B_0), \tag{3.21a}$$

$$B_1 = \frac{3^{2/3} K x^{1/3} e^{-Kt}}{\alpha \Gamma(2/3)}\left(t + \frac{e^{-Kt} - 1}{K\alpha}\right), \tag{3.21b}$$

where we have used Eqs. (3.19) and (3.15).

The t term in Eq. (3.21b) is a secular one due to the forcing of the operator in Eq. (3.21a). Thus for $t = O(\mathrm{Da}^{-1})$, the second term in the expansion (3.13) would be comparable in size to the first term. Therefore, a multiple-scale expansion is desirable, and hence we should use Eq. (3.21b) as an aid in determining the parameters only for times that are $o(\mathrm{Da}^{-1})$. Unfortunately, the results of the multiple-scale expansion will not be particularly illuminating, and thus we also construct the next-order correction to the averaged quantity:

$$\bar{B}_1(t) = \frac{x_{\max}^{4/3} - x_{\min}^{4/3}}{x_{\max} - x_{\min}} \frac{3^{5/3} K \mathrm{e}^{-Kt}}{4\alpha \Gamma(2/3)} \left(t + \frac{\mathrm{e}^{-Kt} - 1}{K\alpha} \right). \tag{3.22}$$

To suppress the secularity in Eq. (3.21b), we introduce the new variables

$$\tau = \mathrm{Da}t, \quad T = [1 + O(\mathrm{Da}^2)]t, \quad C_{\mathrm{k}}(x, \eta, t) = \mathrm{Da}c_1(x, \eta, \tau, T) + o(\mathrm{Da}),$$

$$B_{\mathrm{k}}(x, t) = b_0(x, \tau, T) + \mathrm{Da}b_1(x, \tau, T) + o(\mathrm{Da}).$$

Since to leading order the analyte concentration is still undisturbed, we see that (3.14a) holds with the partial derivative with respect to t replaced by a partial derivative with respect to T, and hence (3.15) becomes

$$b_0(x, \tau, T) = a(x, \tau)\mathrm{e}^{-KT}, \qquad a(x, 0) = \frac{1}{\alpha}. \tag{3.23}$$

The solution steps proceed as above; the expression analogous to (3.20) is

$$\frac{1}{1 - b_0} \left(\frac{\partial b_1}{\partial T} + \frac{\partial b_0}{\partial \tau} + K b_1 \right) = \frac{K}{3^{1/3} \Gamma(2/3)} \int_0^x b_0(x - \xi, \tau, T) \frac{d\xi}{\xi^{2/3}}, \tag{3.24}$$

where the effect of the two time scales may be seen on the left-hand side. Rewriting (3.24), we obtain the following:

$$\frac{\partial b_1}{\partial T} + K b_1 = \mathrm{e}^{-KT} \left[-\frac{\partial a}{\partial \tau} + \frac{K}{3^{1/3} \Gamma(2/3)} \int_0^x \frac{a(x - \xi, \tau)}{\xi^{2/3}} d\xi \right] + \cdots,$$

where the unlisted terms do not contribute to the secularity. Suppressing the secularity, we obtain

$$a(x, \tau) = \frac{1}{\alpha} \sum_{n=0}^{\infty} \frac{(r\tau x^{1/3})^n}{\Gamma(1 + n/3)\, n!}, \qquad r = \frac{K\Gamma(1/3)}{3^{1/3}\Gamma(2/3)}. \tag{3.25}$$

Though $a(x, \tau)$ is exponentially growing in τ, when combined with Eq. (3.23) and written in the original variables, we see that the solution

behaves like

$$e^{-(K-m\mathrm{Da})t}, \qquad t \to \infty,$$

for some positive constant m, which obviously decays. We note that if we substitute Eq. (3.25) into Eq. (3.23) and retain the first two terms for small τ, the results replicate the divergent behavior in Eq. (3.21b) as well as the expression for B_0 previously given in Eq. (3.15).

For comparisons with experimental data, we must calculate $\bar{b}_0$, which is found using Eq. (3.23):

$$\bar{b}_0(\tau, T) = \frac{\mathscr{I}[a; x_{\max}] - \mathscr{I}[a; x_{\min}]}{x_{\max} - x_{\min}} e^{-KT}, \qquad \mathscr{I}[f; x] \equiv \int_0^x f(\xi)\, d\xi. \tag{3.26a}$$

$\mathscr{I}[a; x]$ is easily calculated using Eq. (3.25):

$$\mathscr{I}[a; x] = \frac{x}{\alpha} \sum_{n=0}^{\infty} \frac{(r\tau x^{1/3})^n}{\Gamma(2 + n/3)\, n!}. \tag{3.26b}$$

Because of the complicated nature of Eq. (3.26b), it is best to revert to Eqs. (3.15) and (3.22) when actually calculating parameter values. We generate the graphs for $t = o(\mathrm{Da}^{-1})$ with the first two terms of the expansion given by Eqs. (3.15) and (3.22).

Figure 1 shows a graph of $\bar{B}_0$ [as given by Eq. (3.15)] vs. the *dimensional* time $\tilde{t}$ (in seconds), since this is how the constants would be determined in a given experiment. [The conversion between t and $\tilde{t}$ is given in Eq. (3.6a).] The parameters used are listed in Table 1; they are the same as in [1].

Figure 2 illustrates the differences between the regular and multiple-scale expansions. The thin line is the correction to $\bar{B}_0$ from the regular expansion, given by $\mathrm{Da}\bar{B}_1$ in Eq. (3.22). The correction to $\bar{B}_0$ from the multiple-scale expansion is $\bar{b}_0 - \bar{B}_0$. The thick line is the graph of this quantity as given by Eq. (3.26a) using the first six terms of Eq. (3.26b).

3.2. Case 3a (Da = O(1), $D_D \ll 1$)

As mentioned earlier, to obtain accurate measurements, R_T (and hence Da) must be increased. Often, this forces Da to be $O(1)$. In this case, reaction and diffusion balance. The solution proceeds in an analogous way as above [1]. In particular, we may consider C_1 to be analogous to C_k, and the analogue of Eq. (3.20) is given by

$$\frac{1}{1 - B_k}\left(\frac{\partial B_k}{\partial t} + KB_k\right) = -\frac{\mathrm{Da}}{3^{1/3}\Gamma(2/3)} \int_0^x \frac{\partial B_k}{\partial t}(x - \xi, t)\, \frac{d\xi}{\xi^{2/3}}. \tag{3.27}$$

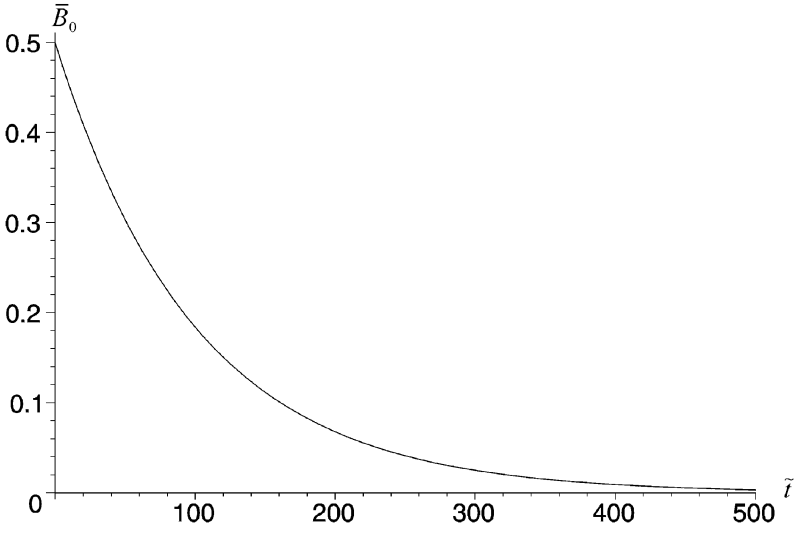

Fig. 1. Leading-order average bound state concentration ($\bar{B}_0$) vs. dimensional time ($\tilde{t}$).

Table 1. Parameter values

Given		*Calculated*	
Parameter	Value	Parameter	Value
Necessary parameters			
C_T (mol/cm^3)	10^{-10}	r	1.37
Da	10^{-1}	T	$10^{-2}\,\tilde{t}/s$
K	1	t	$10^{-2}\,\tilde{t}/s$
$\tilde{k}_a$ (cm^3 mol^{-1} s^{-1})	10^8	α	2
x_{max}	7.92×10^{-1}	γ	1.37×10^{-1}
x_{min}	2.08×10^{-1}	δ	1.20×10^{-1}
		τ	$10^{-3}\,\tilde{t}/s$
Ancillary parameters			
$\tilde{D}$ (cm^2/s)	2.8×10^{-7}	D	5.25×10^{-4}
h (cm)	5×10^{-3}	D_D	6.85×10^{-2}
Pe	1.49×10^{3}	Da_c	1.56
ε	2.08×10^{-2}	$\tilde{k}_d$ (s^{-1})	10^{-2}
		R_T (mol/cm^2)	6.39×10^{-13}

In the limit that Da $\to 0$, Eq. (3.27) reduces to the evolution equation (3.14a) for B_0, as expected.

Equation (3.27) is a variant of a nonlinear Abel equation. Unfortunately, due to the singular nature of the kernel, standard techniques of analysis fail. Therefore, we again use an asymptotic solution. The

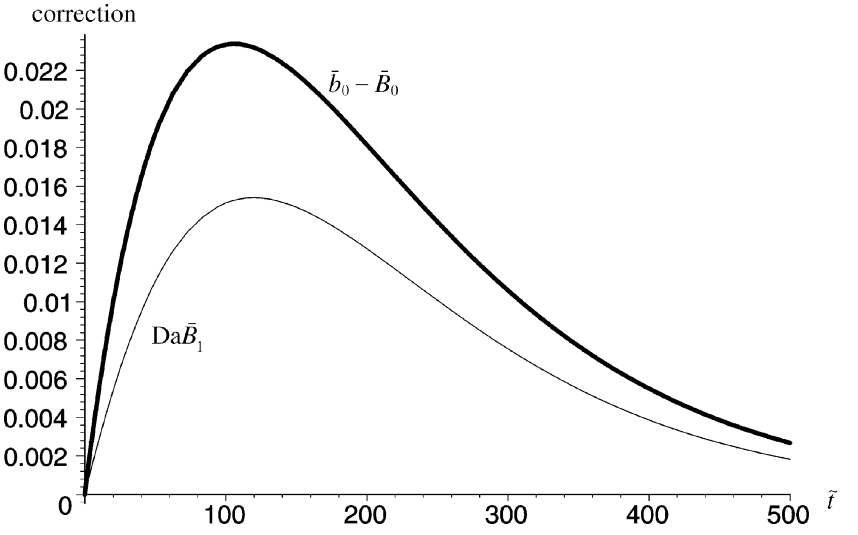

Fig. 2. Correction to $\bar{B}_0$ from uniform expansion ($\bar{b}_0$, thick line) and next term in regular expansion ($\bar{B}_1$, thin line) vs. $\tilde{t}$.

details of the calculations are given in [1]; we adapt them for use here. In the association problem, Edwards assumes a solution of the form

$$B_{\mathrm{k}}(x, t) = \beta_1(x)t + o(t),$$

where $\beta_1(x)$ is the deviation of the solution from the initial condition (zero in the association problem). Motivated by this, in our problem we assume a solution of the form

$$B_{\mathrm{k}}(x, t) = \frac{1}{\alpha} - \beta_1(x)t + o(t).$$

Note that again, $\beta_1(x)$ is the deviation of the solution from the initial condition. After careful calculation, one finds that the β_1 functions for both problems are identical!

This rather surprising result can be explained by noting that in both systems the bound state is being disturbed either by a (dimensionless) value of the analyte of 1 or 0. Thus, either the association or dissociation process proceeds (at least initially) unencumbered by changes in the analyte concentration due to transport.

Since the initial state is given by $1/\alpha$, we may use it to obtain the value of K. However, K is only the ratio of the rate constants. In order to calculate both rate constants individually, we construct a linear fit for the absolute value of the slope S of the small-time data measurements. This fit will then yield $\tilde{k}_{\mathrm{a}}$. Then using our value for K, we may calculate $\tilde{k}_{\mathrm{d}}$.

Due to the similarities in the underlying expressions, the asymptotes of S for small and large $\tilde{k}_a$ are as given in [1], but we must reinterpret them in the dissociation context:

$$S \sim \frac{\tilde{k}_d}{K+1}, \quad \tilde{k}_a \to 0. \tag{3.28}$$

Note that for fixed finite K, $S \to 0$ as $\tilde{k}_a \to 0$ since K is the ratio of the rate constants. Equation (3.28) merely shows that if there is no forward reaction ($\tilde{k}_a = 0$), then the bound state will decay in a purely exponential way. This may be confirmed by expanding Eq. (3.15) for small t and retaining the first two terms; the absolute value of the slope of the resulting linear approximation is given by Eq. (3.28).

For large $\tilde{k}_a$, the asymptote is

$$S \sim \frac{3^{4/3} C_T V^{1/3} \tilde{D}^{2/3} (x_{max}^{2/3} - x_{min}^{2/3})}{2\Gamma(1/3) R_T L^{1/3} h^{1/3} (x_{max} - x_{min})}, \quad \tilde{k}_a \to \infty. \tag{3.29}$$

Therefore, due to the finite rate of transport of dissociated analyte from the unstirred layer, there is a finite limit to the speed at which the reaction can proceed. The limit is independent of any of the rate constants in the problem since it is dependent on the speed of the transport.

4. Effective rate constants

4.1. Dissociation

To interpret the effects of transport more carefully, we approximate the evolution equation for B in a way that yields effective rate constants. To do so, we introduce the following new variables:

$$\gamma = -\frac{\mathrm{Da}\,\mathrm{Ai}(0)}{\mathrm{Ai}'(0)} = \mathrm{Da}_c \mathrm{Pe}^{-1/3}, \qquad \mathrm{Da}_c = \frac{\tilde{k}_a R_T}{\tilde{D}/h}\left[\frac{\Gamma(1/3)}{3^{1/3}\Gamma(2/3)}\right], \tag{4.1}$$

$$z = \gamma^3 x = \left(\frac{\tilde{k}_a^3 R_T^3 h}{V\tilde{D}^2}\right)\frac{\tilde{x}}{3}\left[\frac{\Gamma(1/3)}{\Gamma(2/3)}\right]^3 = \frac{\mathrm{Da}_c^3}{\mathrm{Pe}}\,\frac{\tilde{x}}{L}, \tag{4.2a}$$

$$\eta_e = \gamma\eta = \frac{\tilde{k}_a R_T}{\tilde{D}}\,\frac{\tilde{y}\Gamma(1/3)}{3^{1/3}\Gamma(2/3)} = \mathrm{Da}_c\,\frac{\tilde{y}}{h}, \tag{4.2b}$$

$$C_k(x, \eta, t) = C_{d,e}(z, \eta_e, t) + o(1), \quad B_k(x, t) = B_{d,e}(z, t) + o(1), \tag{4.3}$$

where $\tilde{x}$ and $\tilde{y}$ are the dimensional measurements along and below the channel ceiling. Here Da_c is the Damköhler number for the convective

region and the subscript "e" refers to the fact that these solutions will be used to interpret effective rate constants. We note from the equalities in Eqs. (4.2) that the actual dimension of the channel (h or L) is no longer in the scaling for the relevant variable. Thus, we have now discarded geometric scalings for ones associated with the dynamics of the system.

Substituting Eqs. (4.1)–(4.3) into Eqs. (3.7)–(3.11), we obtain, to leading orders,

$$\frac{\partial^2 C_{\mathrm{d,e}}}{\partial \eta_{\mathrm{e}}^2} = \eta_{\mathrm{e}} \frac{\partial C_{\mathrm{d,e}}}{\partial z}, \tag{4.4}$$

$$C_{\mathrm{d,e}}(0, \eta_{\mathrm{e}}, t) = 0, \tag{4.5}$$

$$\frac{\partial C_{\mathrm{d,e}}}{\partial \eta_{\mathrm{e}}}(z, 0, t) = -\frac{\mathrm{Ai}'(0)}{\mathrm{Ai}(0)} \frac{\partial B_{\mathrm{d,e}}}{\partial t}, \tag{4.6a}$$

$$C_{\mathrm{d,e}}(z, 0, t) = \frac{1}{1 - B_{\mathrm{d,e}}} \left(\frac{\partial B_{\mathrm{d,e}}}{\partial t} + K B_{\mathrm{d,e}} \right) \equiv g(z, t), \tag{4.6b}$$

$$C_{\mathrm{d,e}}(z, \infty, t) = 0, \tag{4.7}$$

$$B_{\mathrm{d,e}}(z, 0) = \frac{1}{\alpha}. \tag{4.8}$$

In order for a matching condition like Eq. (4.7) to be a valid condition for our physical system, η_{e} must be a boundary-layer variable. Hence, we must have that $\mathrm{Da_c} \gg 1$. In Eq. (4.4), time evolution of the analyte concentration has been neglected. For this to be a valid approximation, we must have that $D_{\mathrm{D}} \ll 1.88\mathrm{Da}$. We note from Table 1 that both of these conditions are satisfied only weakly. However, we shall show in this section that even in this case we obtain highly accurate solutions.

As in Sect. 3.1, we take a Laplace transform of Eqs. (4.4) and (4.6a) in the z-direction subject to Eq. (4.5). The solution in Laplace-transform space is proportional to an Airy function (this is why Eq. (4.6a) is scaled to have the peculiar coefficient on the right-hand side). We introduce the following notation for the Laplace transform:

$$\hat{f}(s) = \int_0^\infty f(z) \mathrm{e}^{-sz}\, dz, \qquad f(z) = \frac{1}{2\pi i} \int_{\mathscr{C}} \hat{f}(s) \mathrm{e}^{sz}\, ds,$$

where $\mathscr{C}$ is the Bromwich contour. The solution of this system is

$$\hat{C}_{\mathrm{d,e}}(s, 0, t) = -\frac{1}{s^{1/3}} \frac{d\hat{B}_{\mathrm{d,e}}}{dt}. \tag{4.9}$$

Substituting Eq. (4.9) into the Laplace transform of Eq. (4.6b), we have

$$-\frac{1}{s^{1/3}}\frac{d\hat{B}_{\mathrm{d,e}}}{dt} = \hat{g}. \tag{4.10}$$

We note that Eq. (4.10) is exact in that it follows without approximation once we have reduced to the form Eq. (4.4). Equation (4.10) cannot be inverted in closed form, so we expand $B_{\mathrm{d,e}}$ in a series of powers of $z^{1/3}$:

$$B_{\mathrm{d,e}}(z,t) = \sum_{n=0}^{\infty} z^{n/3} q_{\mathrm{d},n}(t), \qquad q_{\mathrm{d},0}(0) = \frac{1}{\alpha}, \quad q_{\mathrm{d},n}(0) = 0, \tag{4.11}$$

where the initial conditions on $q_{\mathrm{d},n}$ follow from Eq. (4.8). For our series solution to work, z must be small. Though one obvious way to obtain small z is to set Da small (as was done in the previous sections), we see from Eq. (4.2a) that we need not do so.

There is an alternative dominant balance in Eq. (4.10), but it leads to a series that diverges like $z^{-1/3}$ as $z \to 0$. Upon substituting the Laplace transform of Eq. (4.11) into Eq. (4.10) and inverting, we have the following:

$$(1 - B_{\mathrm{d,e}}) \sum_{n=0}^{\infty} \frac{\Gamma(n/3+1) z^{(n+1)/3}}{\Gamma((n+1)/3+1)} \frac{dq_{\mathrm{d},n}}{dt} = -\left(\frac{\partial B_{\mathrm{d,e}}}{\partial t} + K B_{\mathrm{d,e}}\right). \tag{4.12}$$

We note that the left-hand side is $O(z^{1/3})$, and hence to leading order, we have

$$\frac{dq_{\mathrm{d},0}}{dt} + K q_{\mathrm{d},0} = 0, \tag{4.13}$$

which is the same operator as in Eq. (3.14a). Averaging Eq. (4.11), we obtain

$$\bar{B}_{\mathrm{d,e}}(t) = q_{\mathrm{d},0}(t) + \sum_{n=1}^{\infty} \delta_n q_{\mathrm{d},n}(t), \qquad \delta_n = \frac{3(z_{\max}^{n/3+1} - z_{\min}^{n/3+1})}{(n+3)(z_{\max} - z_{\min})}. \tag{4.14}$$

Here δ_n is simply the term that results when we integrate $z^{n/3}$ over the scanning range. The notation δ has been chosen to emphasize that for this expansion to have any utility, the δ_n must be small. Averaging Eq. (4.13), we have the following:

$$\frac{d\bar{B}_{\mathrm{d,e}}}{dt} + K\bar{B}_{\mathrm{d,e}} = O(\delta_1). \tag{4.15}$$

Note that if z is small because Da is small, $O(\delta_1) = O(\mathrm{Da})$.

Continuing to expand Eq. (4.12), we have

$$\frac{z^{1/3}(1-q_{\mathrm{d},0})}{\Gamma(4/3)}\frac{dq_{\mathrm{d},0}}{dt} = 1 - B_{\mathrm{d,e}} - \left(\frac{\partial B_{\mathrm{d,e}}}{\partial t} + KB_{\mathrm{d,e}}\right) + O(z^{2/3}),$$

which, upon averaging, yields

$$\frac{d\bar{B}_{\mathrm{d,e}}}{dt} = -\frac{K\bar{B}_{\mathrm{d,e}}}{1+\delta(1-\bar{B}_{\mathrm{d,e}})} + O(H), \tag{4.16a}$$

$$\delta = \frac{\delta_1}{\Gamma(4/3)} = \frac{9\gamma(x_{\max}^{4/3} - x_{\min}^{4/3})}{4\Gamma(1/3)(x_{\max} - x_{\min})}, \tag{4.16b}$$

$$H = \delta_2 + \delta_1^2 = \gamma^2\left[\frac{3(x_{\max}^{5/3} - x_{\min}^{5/3})}{5(z_{\max} - x_{\min})} + \frac{9(x_{\max}^{4/3} - x_{\min}^{4/3})^2}{16(x_{\max} - x_{\min})^2}\right]. \tag{4.16c}$$

The first term in H comes from the averaging of the $O(z^{2/3})$ term; the second arises from the product of errors in the expression for $\bar{B}_{\mathrm{d,e}}(1-\bar{B}_{\mathrm{d,e}})$. Note that if z is small because Da is small, $O(H) = O(\mathrm{Da}^2)$.

We note that the δ term in Eq. (4.16a) describes the effect on the evolution of the bound state caused by the fact that the analyte is not in equilibrium at the concentration zero. As the bound state dissociates, the analyte concentration is small, but nonzero, in the unstirred layer. Thus, there is a small possibility for rebinding. Therefore, the equilibrium constant K is reduced by a factor of $1+\delta(1-\bar{B}_{\mathrm{d,e}})$. Transforming to dimensional parameters, one sees that determining $\tilde{k}_{\mathrm{d}}$ by fitting the standard model (4.13) to dissociation data will lead to an underestimate of the dissociation rate constant by the same factor.

The $1-\bar{B}_{\mathrm{d,e}}$ term is the average concentration of vacant receptor sites available for rebinding. Lastly, we note that Eq. (4.16a) may be rewritten as

$$\frac{d\bar{B}_{\mathrm{d,e}}}{dt} = -K\bar{B}_{\mathrm{d,e}}(1-p) + O(H), \qquad p = \frac{\delta(1-\bar{B}_{\mathrm{d,e}})}{1+\delta(1-\bar{B}_{\mathrm{d,e}})} \tag{4.17}$$

where p is the probability that an analyte that dissociates will rebind to a receptor on the sensor surface rather then be swept out of the flow cell.

We can indeed solve Eq. (4.16a), though the effective rate constant in the interpretation of Eq. (4.16a) was the desired outcome. We denote the exact solution of the operator in Eq. (4.16a) (without the $O(H)$)

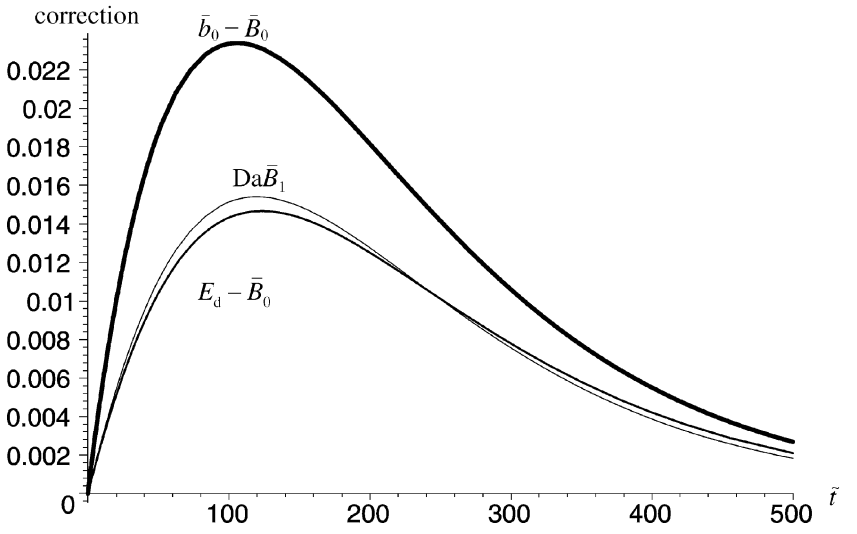

Fig. 3. Correction to $\bar{B}_0$ from $\bar{b}_0$ (thick line), solution of effective rate constant equation (E_d, medium line) and $\bar{B}_1$ (thin line) vs. $\tilde{t}$.

by E_d. Thus we have

$$\frac{dE_\mathrm{d}}{dt} = -\frac{KE_\mathrm{d}}{1+\delta(1-E_\mathrm{d})}, \tag{4.18a}$$

$$\mathrm{e}^{-\delta(E_\mathrm{d}-1/\alpha)}(\alpha E_\mathrm{d})^{1+\delta} = \mathrm{e}^{-Kt}, \tag{4.18b}$$

where we have used Eq. (4.8). Since $B_{\mathrm{d,e}}$ is independent of z to leading order, we note that E_d will provide the first *two* orders of the solution. Unfortunately, due to the $z^{1/3}$ dependence of the next term for $B_{\mathrm{d,e}}$, a simple ODE cannot be derived which is asymptotic to third order. However, as will be shown in the next section, Eq. (4.18b) actually approximates the solution quite well to the first *three* orders.

We now analyze the correction to $\bar{B}_0$ given by E_d. Using the parameters in Table 1, Fig. 3 is a replot of Fig. 1 with the addition of the plot of the correction $E_\mathrm{d} - \bar{B}_0$, indicated by the line of medium thickness. Note that, as expected, all corrections are $O(\mathrm{Da})$.

4.2. Association

We repeat the analysis in Sect. 4.1 for association kinetics. The general formulation of the problem is discussed in detail in [1]; we merely extract those portions of the analysis relevant for the work at hand. During association kinetics, $C(0, y) = 1$ since we choose to normalize

the dimensional analyte concentration by the upstream value. Therefore, the zeroes in the boundary and matching conditions (4.5) and (4.7) are replaced by ones. These changes roughly mean that the sum of the dissociaion analyte solution and the association analyte solution is 1. This causes an adjustment in our definition of the Dirichlet condition g, and the analogue of Eq. (4.12) is given by

$$(1 - B_{a,e}) \sum_{n=0}^{\infty} \frac{\Gamma(n/3 + 1) z^{(n+1)/3}}{\Gamma((n+1)/3 + 1)} \frac{dq_{a,n}}{dt} = 1 - B_{a,e} - \left(\frac{\partial B_{a,e}}{\partial t} + K B_{a,e} \right). \tag{4.19}$$

Following the steps in Sect. 4.1, to leading order we obtain

$$\frac{dq_{a,0}}{dt} + K q_{a,0} = 1 - q_{a,0},$$

the averaged first-order equation is

$$\frac{d\bar{B}_{a,e}}{dt} + \alpha \bar{B}_{a,e} = 1 + O(\delta_1), \tag{4.20a}$$

and the averaged second-order equation is the following:

$$\frac{d\bar{B}_{a,e}}{dt} = \frac{1 - \alpha \bar{B}_{a,e}}{1 + \delta(1 - \bar{B}_{a,e})} + O(H). \tag{4.20b}$$

After a suitable change in notation, Eq. (4.20b) with $x_{\min} = 0$ and $x_{\max} = 1$ agrees with Eqs. (32a) and (32b) in Mason *et al.* [6]

The initial condition for $B_{a,e}$ may be arbitrary, but we choose the physically realizable case where it is uniformly zero. With this initial condition, we may solve Eq. (4.20b) (without the $O(H)$); denoting the solution by E_a, we have

$$e^{-\delta E_a} (1 - \alpha E_a)^{1 + \delta\chi} = e^{-\alpha t}, \qquad \chi = \frac{K}{\alpha}. \tag{4.21}$$

The agreement between E_a and the association solution is similar to that shown in Sect. 4.1 for the dissociation kinetics; this will be shown in more detail in Sect. 5.2.

5. Series solutions

5.1. Dissociation

In order to ascertain the accuracy of the evolution equation (4.16a), we construct series solutions for $B_{d,e}$. By substituting Eq. (4.11) into

Eq. (4.12), we obtain the following series of equations:

$$\sum_{n=0}^{\infty} z^{n/3}\left[\frac{dq_{\mathrm{d},n}}{dt}+Kq_{\mathrm{d},n}\right]=z^{1/3}\left[\sum_{n=0}^{\infty} z^{n/3}\sum_{j=0}^{n}\frac{\Gamma(j/3+1)}{\Gamma((j+1)/3+1)}q^{*}_{\mathrm{d},n-j}\frac{dq_{\mathrm{d},j}}{dt}\right], \tag{5.1a}$$

$$q^{*}_{\mathrm{d},n}(t)=\begin{cases} q_{\mathrm{d},0}(t)-1, & n=0,\\ q_{\mathrm{d},n}(t), & \text{else.}\end{cases} \tag{5.1b}$$

The right-hand side of Eq. (5.1a) is always known, since due to the presence of the extra $z^{1/3}$ term, these are forcing terms to the operator on the left-hand side, which appears at all orders.

In particular, we generate the first three terms in the expansion:

$$\frac{dq_{\mathrm{d},0}}{dt}+Kq_{\mathrm{d},0}=0, \tag{5.2a}$$

$$\frac{dq_{\mathrm{d},1}}{dt}+Kq_{\mathrm{d},1}=\frac{1}{\Gamma(4/3)}(q_{\mathrm{d},0}-1)\frac{dq_{\mathrm{d},0}}{dt}, \tag{5.2b}$$

$$\frac{dq_{\mathrm{d},2}}{dt}+Kq_{\mathrm{d},2}=\frac{1}{\Gamma(4/3)}q_{\mathrm{d},1}\frac{dq_{\mathrm{d},0}}{dt}+\frac{\Gamma(4/3)}{\Gamma(5/3)}(q_{\mathrm{d},0}-1)\frac{dq_{\mathrm{d},1}}{dt}. \tag{5.2c}$$

Solving Eq. (5.2a) subject to the initial condition in Eq. (4.11), we have

$$q_{\mathrm{d},0}(t)=\frac{\mathrm{e}^{-Kt}}{\alpha}, \tag{5.3}$$

which of course matches with Eq. (3.15). Substituting Eq. (5.3) into Eq. (5.2b) and solving, we obtain the following:

$$q_{\mathrm{d},1}(t)=\frac{\chi\mathrm{e}^{-Kt}}{\Gamma(4/3)}\left(t+\frac{\mathrm{e}^{-Kt}-1}{K\alpha}\right), \tag{5.4}$$

where we have used the initial condition in Eq. (4.11). We note that Eq. (5.4) agrees with Eq. (3.21b).

Substituting Eqs. (5.3) and (5.4) into Eq. (5.2c) and using the initial condition in Eq. (4.11), we obtain

$$\begin{aligned} q_{\mathrm{d},2}(t)=\frac{\chi\mathrm{e}^{-Kt}}{\alpha\Gamma(4/3)}\Bigg\{&\frac{\mathrm{e}^{-2Kt}-1}{K\alpha}\left[\frac{1}{2\Gamma(4/3)}+\frac{\Gamma(4/3)}{\Gamma(5/3)}\right]\\ &+\frac{(\alpha t+1)\mathrm{e}^{-Kt}-1}{\alpha}\left[\frac{1}{\Gamma(4/3)}+\frac{\Gamma(4/3)}{\Gamma(5/3)}\right]\\ &+\frac{\Gamma(4/3)}{\Gamma(5/3)}\left[-t(\alpha+1)+\frac{K\alpha t^{2}}{2}+\frac{3(1-\mathrm{e}^{-Kt})}{K}\right]\Bigg\}. \end{aligned} \tag{5.5}$$

From Eq. (4.14) we have that the averaged expression is given by

$$\bar{B}_{\mathrm{d,e}}(t) = q_{\mathrm{d},0}(t) + O(\delta_1), \tag{5.6a}$$

$$= q_{\mathrm{d},0}(t) + \delta_1 q_{\mathrm{d},1}(t) + O(\delta_2), \tag{5.6b}$$

$$= q_{\mathrm{d},0}(t) + \delta_1 q_{\mathrm{d},1}(t) + \delta_2 q_{\mathrm{d},2}(t) + O(z_{\max} + z_{\min}). \tag{5.6c}$$

We now examine the behavior of the second-order correction term $\delta_2 q_{\mathrm{d},2}$. Figure 4 shows the graph of $\delta_2 q_{\mathrm{d},2}$ as a thin line. The thick line is the correction to $q_{\mathrm{d},0} + \delta_1 q_{\mathrm{d},1}$ from using E_{d}. Note the similarity between the two graphs. Motivated by this fact, in Fig. 5 we graph the difference between E_{d} and $q_{\mathrm{d},0} + \delta_1 q_{\mathrm{d},1} + \delta_2 q_{\mathrm{d},2}$. Note the incredibly close agreement.

Why is the agreement so close? Inspired by Eq. (4.14), we expand the first three terms of E_{d} as

$$E_{\mathrm{d}}(t) = E_{\mathrm{d},0}(t) + \delta_1 E_{\mathrm{d},1}(t) + \delta_2 E_{\mathrm{d},2} + O(\delta_3). \tag{5.7}$$

Substituting this series into Eq. (4.18a), we obtain, to leading three orders,

$$\frac{dE_{\mathrm{d},0}}{dt} + KE_{\mathrm{d},0} = 0, \tag{5.8a}$$

$$\frac{dE_{\mathrm{d},1}}{dt} + KE_{\mathrm{d},1} = -\frac{1}{\Gamma(4/3)}(1 - E_{\mathrm{d},0})\frac{dE_{\mathrm{d},0}}{dt}, \tag{5.8b}$$

$$\frac{dE_{\mathrm{d},2}}{dt} + KE_{\mathrm{d},2} = \left(\frac{\delta_1^2}{\delta_2}\right)\frac{1}{\Gamma(4/3)}(E_{\mathrm{d},0} - 1)\frac{dE_{\mathrm{d},1}}{dt} + \left[\frac{\delta_1^2}{\delta_2}\frac{\Gamma(5/3)}{\Gamma^2(4/3)}\right]\frac{\Gamma(4/3)}{\Gamma(5/3)}E_{\mathrm{d},1}\frac{dE_{\mathrm{d},0}}{dt}, \tag{5.8c}$$

where the balance in Eq. (5.8c) comes from the fact that when Da is small (as in Figs. 4 and 5), $\delta_1^2 = O(\delta_2)$. The operators in Eqs. (5.8a) and (5.8b) are exactly those in Eqs. (5.2a) and (5.2b), as they should be.

To examine the difference between Eqs. (5.8c) and (5.2c), we simplify our coefficient δ_1^2/δ_2, yielding

$$\frac{\delta_1^2}{\delta_2} = \frac{15}{16}\left[1 - x_{\min}x_{\max}\left(\frac{x_{\max}^{1/3} - x_{\min}^{1/3}}{x_{\max}^{4/3} - x_{\min}^{4/3}}\right)^2\right]^{-1}. \tag{5.9}$$

Therefore, we see that $\delta_1^2/\delta_2 \geqq 15/16$. To obtain an upper bound, we examine the physically realizable case where the scanner is symmetric: that is, when $x_{\min} = 1 - x_{\max}$. By symmetry arguments it is easy to see that an extremum will be reached when $x_{\min} = x_{\max} = 1/2$, and that

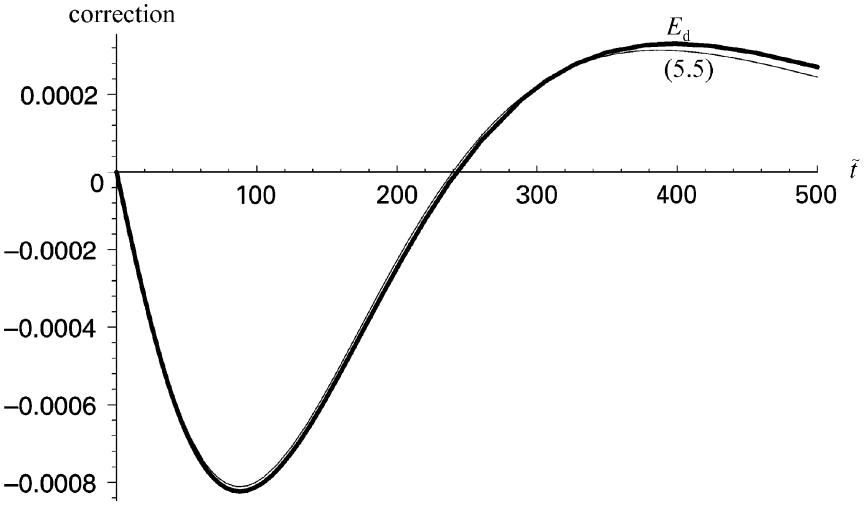

Fig. 4. Second-order correction to series solution Eq. (5.6b) from series ($\delta_2 q_{d,2}$, thin line) and E_d (thick line) vs. $\tilde{t}$.

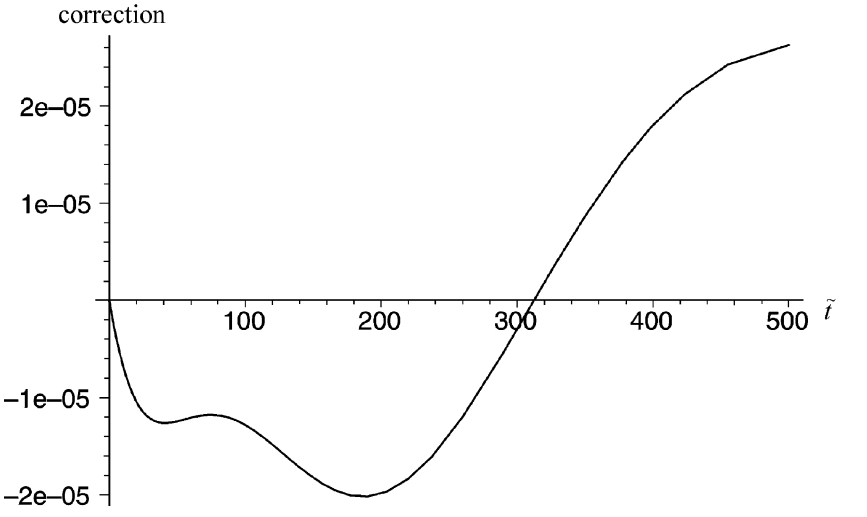

Fig. 5. Third-order correction to series solution Eq. (5.6c) from E_d vs. $\tilde{t}$.

extremal value is given by

$$\lim_{\substack{x_{\min}\to 1/2^- \\ x_{\max}\to 1/2^+}} \frac{\delta_1^2}{\delta_2} = 1.$$

Using this result, we obtain the following bounds:

$$\frac{15}{16} \leqq \frac{\delta_1^2}{\delta_2} \leqq 1, \qquad 1.06 \leqq \frac{\delta_1^2 \Gamma(5/3)}{\delta_2 \Gamma^2(4/3)} \leqq 1.13.$$

Hence, due to the forms of the coefficients, E_d approximates the true solution even more accurately than the order estimates indicate. Using the parameters in Table 1, we have that

$$\frac{\delta_1^2}{\delta_2} = 9.86 \times 10^{-1}, \qquad \frac{\delta_1^2}{\delta_2}\frac{\Gamma(5/3)}{\Gamma^2(4/3)} = 1.12,$$

which explains the close agreement in Figs. 4 and 5.

5.2. *Association*

For the association kinetics, the analogue of Eq. (5.1a) is given by

$$\sum_{n=0}^{\infty} z^{n/3}\left[\frac{dq_{a,n}}{dt} + \alpha q_{a,n}\right] = 1 + z^{1/3}\left[\sum_{n=0}^{\infty} z^{n/3} \sum_{j=0}^{n} \frac{\Gamma(j/3+1)}{\Gamma((j+1)/3+1)} q^*_{a,n-j}\frac{dq_{a,j}}{dt}\right].$$

Generating the first three terms in the expansion, we have the following:

$$\frac{dq_{a,0}}{dt} + \alpha q_{a,0} = 1, \tag{5.10a}$$

$$\frac{dq_{a,1}}{dt} + \alpha q_{a,1} = \frac{1}{\Gamma(4/3)}(q_{a,0} - 1)\frac{dq_{a,0}}{dt}, \tag{5.10b}$$

$$\frac{dq_{a,2}}{dt} + \alpha q_{a,2} = \frac{1}{\Gamma(4/3)} q_{a,1}\frac{dq_{a,0}}{dt} + \frac{\Gamma(4/3)}{\Gamma(5/3)}(q_{a,0} - 1)\frac{dq_{a,1}}{dt}. \tag{5.10c}$$

Solving Eqs. (5.10a) and (5.10b) subject to the zero initial condition discussed earlier, we obtain

$$q_{a,0}(t) = \frac{1 - e^{-\alpha t}}{\alpha}, \tag{5.11a}$$

$$q_{a,1}(t) = \frac{e^{-\alpha t}}{\alpha\Gamma(4/3)}\left(\frac{e^{-\alpha t} - 1}{\alpha} - Kt\right). \tag{5.11b}$$

Substituting Eqs. (5.11) into Eq. (5.10c), we have

$$\begin{aligned} q_{a,2}(t) = \frac{e^{-\alpha t}}{\alpha\Gamma(4/3)}\Bigg\{ & \frac{1 - e^{-2\alpha t}}{\alpha^2}\left[\frac{1}{2\Gamma(4/3)} + \frac{\Gamma(4/3)}{\Gamma(5/3)}\right] \\ & + \frac{(Kt+1)e^{-\alpha t} - 1}{\alpha}\left[\frac{1}{\Gamma(4/3)} + \frac{\Gamma(4/3)}{\Gamma(5/3)}\right] \\ & + \frac{\Gamma(4/3)}{\alpha\Gamma(5/3)}\left[K(K-1)t - \frac{K^2\alpha t^2}{2} + \frac{3K(1 - e^{-\alpha t})}{\alpha}\right]\Bigg\}, \end{aligned} \tag{5.12}$$

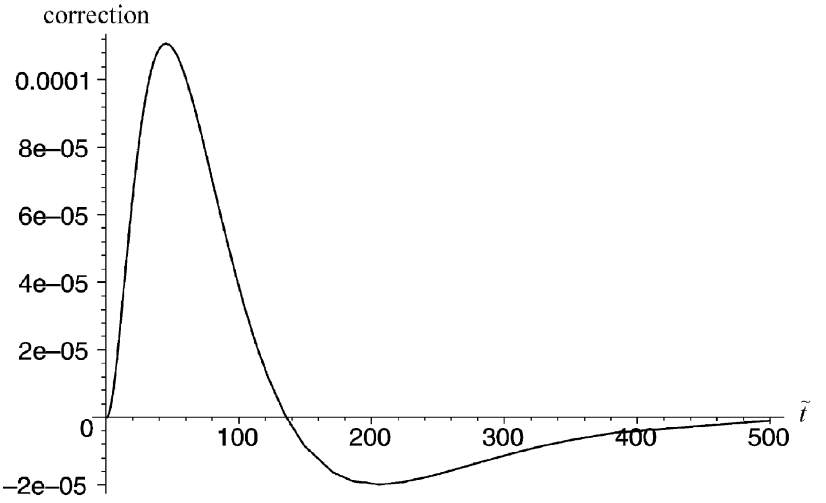

Fig. 6. Correction to first three terms of averaged series solution $\bar{B}_{a,e}$ from effective rate constant equation solution E_a vs. $\tilde{t}$.

and using these expressions in Eqs. (5.6) (with the subscript "d" replaced by "a") will yield the appropriate expressions for $\bar{B}_{a,e}$.

If we check the agreement of E_a to the first three terms in our expansion for $\bar{B}_{a,e}$, we obtain the following three equations:

$$\frac{dE_{a,0}}{dt} + \alpha E_{a,0} = 1, \tag{5.13a}$$

$$\frac{dE_{a,1}}{dt} + \alpha E_{a,1} = -\frac{1}{\Gamma(4/3)}(1 - E_{a,0})\frac{dE_{a,0}}{dt}, \tag{5.13b}$$

$$\frac{dE_{a,2}}{dt} + \alpha E_{a,2} = \left(\frac{\delta_1^2}{\delta_2}\right)\frac{1}{\Gamma(4/3)}(E_{a,0} - 1)\frac{dE_{a,1}}{dt} + \left[\frac{\delta_1^2}{\delta_2}\frac{\Gamma(5/3)}{\Gamma^2(4/3)}\right]\frac{\Gamma(4/3)}{\Gamma(5/3)}E_{a,1}\frac{dE_{a,0}}{dt}, \tag{5.13c}$$

where the form of the series is as in Eq. (5.7) and the solution process is as in Sect. 5.1. Therefore, we have the same close agreement, as shown in Fig. 6.

5.3. Comparison with numerical results

In order to verify our analytical results, we compare our work with numerical simulations of the problem. In particular, we compare our

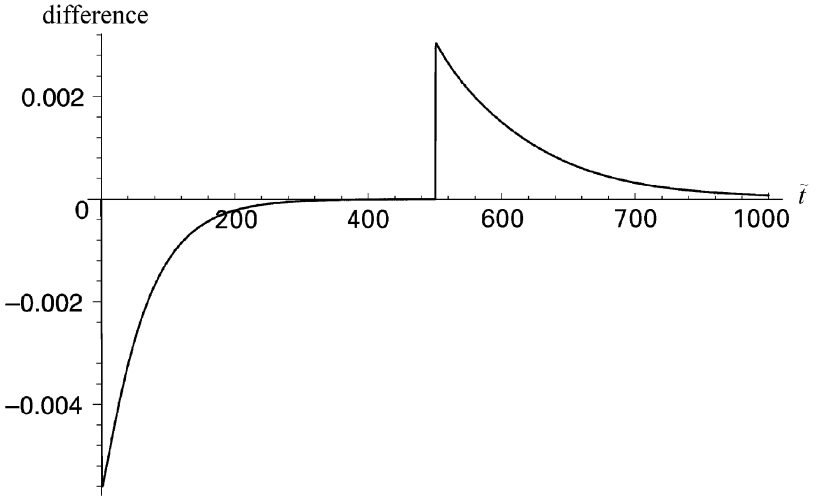

Fig. 7. Difference between three-term series and numerical solution vs. $\tilde{t}$.

work with results from the numerical code in [6]. This code solves the full convection-diffusion system (2.1)–(2.6) using the method of lines. We compare our work with a solution on a 96×96 grid, which corresponds to a second-order error of approximately 10^{-4}. The code runs two simulations: an association experiment immediately followed by a dissociation experiment.

To run comparisons, we calculated the difference between our three-term series solutions given in Sects. 5.1 and 5.2 and results generated by the numerical code in [6]. The results of the comparison are shown in Fig. 7. The range $\tilde{t} \in [0, 500]$ is the association phase, and $\tilde{t} \in [500, 1000]$ is the dissociation phase. As expected, the difference in the results is $O(z_{\max} + z_{\min}) = O(\mathrm{Da}^3) = O(10^{-3})$.

6. Conclusions

Key to the understanding of certain biological reactions are the values of their association and dissociation rate constants. The advent of SPR technology and its application in the BIAcore™ device have allowed scientists to measure the concentration of bound ligands precisely in real time. However, in order to translate these measurements into useful estimates of the rate constants, accurate mathematical models are needed.

We summarized the relevant mathematical equations for the full system from [1], which involves a convection-diffusion equation with

a boundary reaction. We noted that the key dimensionless group is the Damköhler number Da, which measures the ratio of the time scales of reaction and diffusion. If $\mathrm{Da} \ll 1$, the reaction kinetics decouple from the transport effects and to leading order our model produces the well-known result for a well-mixed system [9]. The form of the next-order correction for small Da suggested a multiple-scale expansion that consists of an infinite series of terms. Both the regular expansion and a truncated version of the multiple-scale expansion provided improved approximate solutions to the full system.

For many reactions of interest, the current SPR technology requires one to work at a relatively high concentration of binding sites in order to obtain accurate measurements of the bound concentration as a function of time. This increase in R_T often forces Da to be $O(1)$. In this case, the kinetic and transport effects are coupled and the nonlinear integrodifferential equation (3.27) results. However, one can obtain important information about the rate constants by examining the small-time linearization of the measured data. We indicated how this small-time solution would change as k_a varied. As $k_a \to 0$, the reaction is governed by a purely dissociative process. As $k_a \to \infty$, the speed of the reaction asymptotes to a finite value governed by the transport process.

By introducing dynamical, as opposed to geometric, scalings, we noted that the resulting operator (4.4) has series solutions in the variable z. We used these series to construct an ordinary differential equation for the evolution of $\bar{B}_e$. This equation is in the form of a standard chemical rate equation but with the rate constants replaced by effective rate coefficients. Not only is the equation easy to solve, but also its coefficients display in a simple way the effects of transport upon the reaction. These effects involve the product of the average fraction of sites available for rebinding $1 - \bar{B}_e$ and a parameter δ which is a ratio of the rate of reaction to the rate of transport. In terms of these quantities, the probability that dissociation of a bound complex will lead to the escape of the analyte from the sensor surface, rather than its return to the surface and its rebinding, is $1 - p = [1 + (1 - \bar{B}_e)\delta]^{-1}$.

In addition, by constructing the actual series solutions in z, we noted that the evolution equation is asymptotic to the true solution to leading two orders and closely approximates the solution to leading three orders. This shows why numerical solutions of the ordinary differential equation with effective rate coefficients agree so well with numerical solutions of the full partial differential equation formulation [6, 8]. In addition, we explicitly compared our results with simulations of the full convection-diffusion system from [6], and found the answers in close agreement.

These results provide a solid framework from which other work can be launched. In particular, the full model should provide information regarding transport effects in more realistic geometries for biological systems.

Acknowledgement. The authors thank Carla Wofsy for helpful discussions regarding this paper.

Nomenclature

Variables and parameters

Units are listed in terms of length (L), moles (N), or time (T). If the same letter appears both with and without tildes, the letter with a tilde has dimensions, while the letter without a tilde is dimensionless. The equation where a quantity first appears is listed, if appropriate.

$a(x, \tau)$: amplitude function in two-time expansion (3.23).
$B(x, t_c)$: bound ligand concentration on channel ceiling $y = 0$ at position x and time t_c (2.5).
$b(x, \tau, T)$: bound ligand concentration in two-time expansion.
$\mathscr{C}$: the Bromwich contour for inversion of a Laplace transform.
$C(x, y, t_c)$: analyte concentration at position (x, y) and time t_c (2.1).
$c(x, \eta, \tau, T)$: analyte concentration in two-time expansion.
$\tilde{D}$: molecular diffusion coefficient, units L^2/T (2.2).
Da: the Damköhler number, which measures the ratio of reaction and diffusion effects.
$E(t)$: solution of the effective rate constant equation (4.18a).
$f(\cdot)$: arbitrary function (3.26a).
$g(z, t)$: arbitrary Dirichlet data (4.6b).
H: error in second-order evolution equation for $\bar{B}_e$ (4.16c).
h: height of the channel, units L.
$\mathscr{I}[\cdot; x]$: integration operator, defined in Eq. (3.26a) as

$$\mathscr{I}[f; x] \equiv \int_0^x f(\xi)\, d\xi.$$

j: indexing variable (5.1a).
$\tilde{K}$: equilibrium dissociation constant for system, defined as $\tilde{k}_d/\tilde{k}_a$, units N/L^3.
$\tilde{k}_a$: binding rate, units $L^3/(NT)$.
$\tilde{k}_d$: dissociation rate, units T^{-1}.

L: length of the channel, units L.
m: arbitrary constant, variously defined.
n: indexing variable (3.25).
Pe: Peclét number for the system, which measures the ratio of convective to diffusive effects, defined as $Vh^2/\tilde{D}L$ (2.1).
p: probability that an analyte molecule that dissociates will rebind to a receptor on the sensor surface rather then be swept out of the flow cell (4.17).
$q_n(t)$: coefficient of $z^{n/3}$ in expansion of B_e (4.11).
R_T: total number of receptor sites, units N/L^2 (2.5).
r: dimensionless parameter, defined in Eq. (3.25) as $\Gamma(1/3)K/3^{1/3}\Gamma(2/3)$.
S: absolute value of the slope of the short-time approximation for the evolution of $\bar{B}_k$.
s: variable in Laplace transform space.
T: variable in two-time expansion, defined as $T = [1 + O(\mathrm{Da}^2)]t$.
$\tilde{t}$: time from beginning of the dissociation experiment, units T.
V: four times the (maximal) velocity of flow at center of channel, units L/T.
$\tilde{x}$: measure of length along the channel, units L.
$\tilde{y}$: measure of height below the binding surface, units L.
$\mathscr{Z}$: the integers.
z: scaled measure of length along the channel, value $\gamma^3 x$ (4.2a).
α: dimensionless constant, defined as $1 + K$ (3.2b).
$\beta_1(x)$: term in expansion of $B_k(x, t)$ for small t.
γ: dimensionless constant (4.1).
δ: dimensionless constant measuring effects of transport (4.14).
ε: aspect ratio of the channel, defined as h/L (2.1).
η: stretched spatial variable in the y-direction, dimensionless (3.3a).
ξ: dummy variable (3.20).
τ: variable in two-time expansion, value $\mathrm{Da}t$.
χ: dimensionless constant, defined as K/α (4.21).

Other notation

a: as a subscript, used to indicate the association process.
c: as a subscript, used to indicate the convective time scale (2.1).

D: as a subscript, refers to variation on the time scale of diffusion near the wall (3.3a).

d: as a subscript, used to indicate the dissociation process.

e: as a subscript, used to indicate effective rate constants (4.2b).

k: as a subscript, refers to variation on the time scale where the reaction causes the evolution of the bound state (3.6b).

max: as a subscript, used to indicate the right endpoint of the scanning range (3.12).

min: as a subscript, used to indicate the left endpoint of the scanning range (3.12).

$n \in \mathscr{L}$: as a subscript, used to indicate an expansion in Da (3.13), z (4.11), or δ_n (5.7).

T: as a subscript, used to indicate the total value of a quantity (2.5).

*: as a superscript, used to indicate a modified version of q (5.1a).

$\bar{}$: used to denote the mean of the bound concentration over a subset of the boundary, defined in Eq. (3.12) as

$$\bar{B}_{\mathrm{k}}(t) = \frac{1}{x_{\max} - x_{\min}} \int_{x_{\min}}^{x_{\max}} B_{\mathrm{k}}(x, t)\, dx.$$

$\hat{}$: used to indicate the Laplace transform of a quantity.

References

1. D. A. Edwards, Estimating rate constants in a convection-diffusion system with a boundary reaction, IMA J. Appl. Math. **63** (1999) 89–112
2. R. Glaser, Antigen-antibody binding and mass transport by convection and diffusion to a surface: A two-dimensional computer model of binding and dissociation kinetics, Anal. Biochem. **213** (1993) 152–161
3. B. Goldstein and M. Dembo, Approximating the effects of diffusion on reversible reactions at the cell surface: Ligand-receptor kinetics, Biophys. J. **68** (1995) 1222–1230
4. R. Karlsson, H. Roos, L. Fägerstam and B. Persson, Kinetic and concentration analysis using BIA technology, Methods **6** (1994) 99–110
5. B. K. Lok, Y.-L. Cheng and C. R. Robertson, Protein adsorption on crosslinked polydimethylsiloxane using total internal reflection fluorescence, J. Coll. Int. Sci. **91** (1983) 104–116
6. T. Mason, A. R. Pineda, C. Wofsy and B. Goldstein, Effective rate models for the analysis of transport-dependent biosensor data, Math. Biosci., in press
7. D. G. Myszka, Kinetic analysis of macromolecular interactions using surface plasmon resonance biosensors, Curr. Opin. Biotech. **8** (1997) 50–57

8. D. G. Myszka, X. He, M. Dembo, T. Morton and B. Goldstein, Extending the range of rate constants available from BIACORE: Intrerpreting mass transport influenced binding data, Biophys. J. **75** (1998) 583–594
9. D. J. O'Shannessy, Determination of kinetic rate and equilibrium binding constants for macromolecular interactions: a critique of the surface plasmon resonance literature, Curr. Opin. Biotech. **5** (1994) 65–71
10. M. Raghavan, M. Y. Chen, L. N. Gastinel and P. J. Bjorkman, Investigation of the interaction between the class I MHC-related Fc receptor and its immunoglobulin ligand, Immunity **1** (1994) 303–315
11. A. Szabo, L. Stolz and R. Granzow, Surface plasmon resonance and its use in biomolecular interaction analysis (BIA), Curr. Opin. Struct. Bio. **5** (1995) 699–705

This article was processed by the author
using the Springer-Verlag TEX PJour1g macro package 1991.